

Effects of $\text{Co}_3(\text{PO}_4)_2$ coatings on $\text{LiNi}_{0.8}\text{Co}_{0.16}\text{Al}_{0.04}\text{O}_2$ cathodes during application of high current

Kwang Sun Ryu · Sang Hyo Lee · Bon Keup Koo ·
Ju Wook Lee · Kwang Man Kim · Yong Joon Park

Received: 8 December 2007 / Revised: 17 April 2008 / Accepted: 21 April 2008 / Published online: 7 May 2008
© Springer Science+Business Media B.V. 2008

Abstract The electrochemical properties of bare and $\text{Co}_3(\text{PO}_4)_2$ -coated $\text{LiNi}_{0.8}\text{Co}_{0.16}\text{Al}_{0.04}\text{O}_2$ electrodes after high current damage testing were characterized. Damage was induced by cycling with a high current density of 600 m Ag^{-1} . $\text{Co}_3(\text{PO}_4)_2$ -coated $\text{LiNi}_{0.8}\text{Co}_{0.16}\text{Al}_{0.04}\text{O}_2$ electrodes exhibit lower capacity loss and better charge retention than bare $\text{LiNi}_{0.8}\text{Co}_{0.16}\text{Al}_{0.04}\text{O}_2$ electrodes after damage testing. The discharge capacity reduction of bare and $\text{Co}_3(\text{PO}_4)_2$ -coated electrodes after damage testing were ~ 27 and 15% , respectively. The impedance of cells containing bare electrodes remarkably increased after high current cycling, which may be induced by damage to the electrode surface. However, damage was successfully suppressed by the $\text{Co}_3(\text{PO}_4)_2$ coating. Bare $\text{LiNi}_{0.8}\text{Co}_{0.16}\text{Al}_{0.04}\text{O}_2$ electrodes developed large amounts of cracks and

other extended defects after high current cycling. In contrast, $\text{Co}_3(\text{PO}_4)_2$ -coated electrodes maintained stable features after high current cycling, indicating the coating layer effectively protected the surface of the $\text{LiNi}_{0.8}\text{Co}_{0.16}\text{Al}_{0.04}\text{O}_2$ powder.

Keywords Chemical synthesis · Electrochemical measurement · Electrochemical properties

1 Introduction

Since the emergence of lithium ion batteries, many efforts have been made to develop good electrode materials with improved electrochemical performance and low material cost. Research has shown that the surface of electrode materials is of great importance to the electrochemical properties of lithium ion batteries. As a result, many groups have focused attention on surface coating the cathode material with metal oxide nanoparticles [1–9]. Coating metal oxides, such as TiO_2 , Al_2O_3 , SiO_2 and AlPO_4 , on the surface improve capacity retention, rate capability, and, in some cases, thermal stability, without sacrificing the specific capacity of the cathode. Recently, $\text{Co}_3(\text{PO}_4)_2$ nanoparticle coatings were introduced for modifying LiCoO_2 [10]. $\text{Co}_3(\text{PO}_4)_2$ nanoparticles completely reacted with Li in LiCoO_2 , resulting in the formation of a LiCoPO_4 phase and a partially lithium-deficient Li_xCoO_2 phase. The olivine LiCoPO_4 phase is very electrochemically and thermally stable, even after full delithiation [11]. Also, a $\text{Co}_3(\text{PO}_4)_2$ coating on the surface of $\text{LiNi}_{0.8}\text{Co}_{0.16}\text{Al}_{0.04}\text{O}_2$ has been reported [12]. In fact, LiNiO_2 -based materials, such as $\text{LiNi}_{0.8}\text{Co}_{0.16}\text{Al}_{0.04}\text{O}_2$, are very promising cathode materials with higher capacity and lower cost than commercial LiCoO_2 for lithium ion batteries [13–18].

K. S. Ryu (✉)
Department of Chemistry, Ulsan University, Moogeo-dong,
Nam-gu, Ulsan 680-749, Korea
e-mail: ryuks@ulsan.ac.kr

S. H. Lee · B. K. Koo
Department of Metallurgical Engineering, Hanbat National
University, Daejeon 305-719, Korea

J. W. Lee
Semiconductor Process Team, Electronics and
Telecommunications Research Institute, Daejeon 305-350,
Korea

K. M. Kim
Ionics Device Team, Electronics and Telecommunications
Research Institute, Daejeon 305-350, Korea

Y. J. Park (✉)
Division of Advanced Industrial Engineering, Kyonggi
University, San94-6, Yiui-dong, Yeongtong-gu, Suwon,
Gyeonggi-do 443-760, Korea
e-mail: yjpark2006@kyonggi.ac.kr

However, LiNiO_2 -based materials rapidly take up moisture and easily form surface film impurities, such as Li_2CO_3 or LiOH [19–21]. The $\text{Co}_3(\text{PO}_4)_2$ coating reacts with such impurities during annealing to form an olivine LiCoPO_4 phase on the surface, which improves storage at high temperature [12].

In the present work, the effects of a $\text{Co}_3(\text{PO}_4)_2$ nanoparticle coating on $\text{Li}[\text{Co}_{0.1}\text{Ni}_{0.15}\text{Li}_{0.2}\text{Mn}_{0.55}]\text{O}_2$ cathode material are characterized for surface damage caused by high current cycling. Currently, cathode materials with high rate capabilities have attracted attention for their potential application in hybrid electric vehicles (HEV) or electric vehicles (EV) [22, 23]. However, the rapid electrochemical reaction due to high current can induce mechanical stress and strain to the oxide particle, which lead to damage to the structural and electrochemical properties. This damage may concentrate on the surface of the particle, thus the $\text{Co}_3(\text{PO}_4)_2$ coating on the surface of the cathode material is expected to effectively depress high current damage to the cathode material itself.

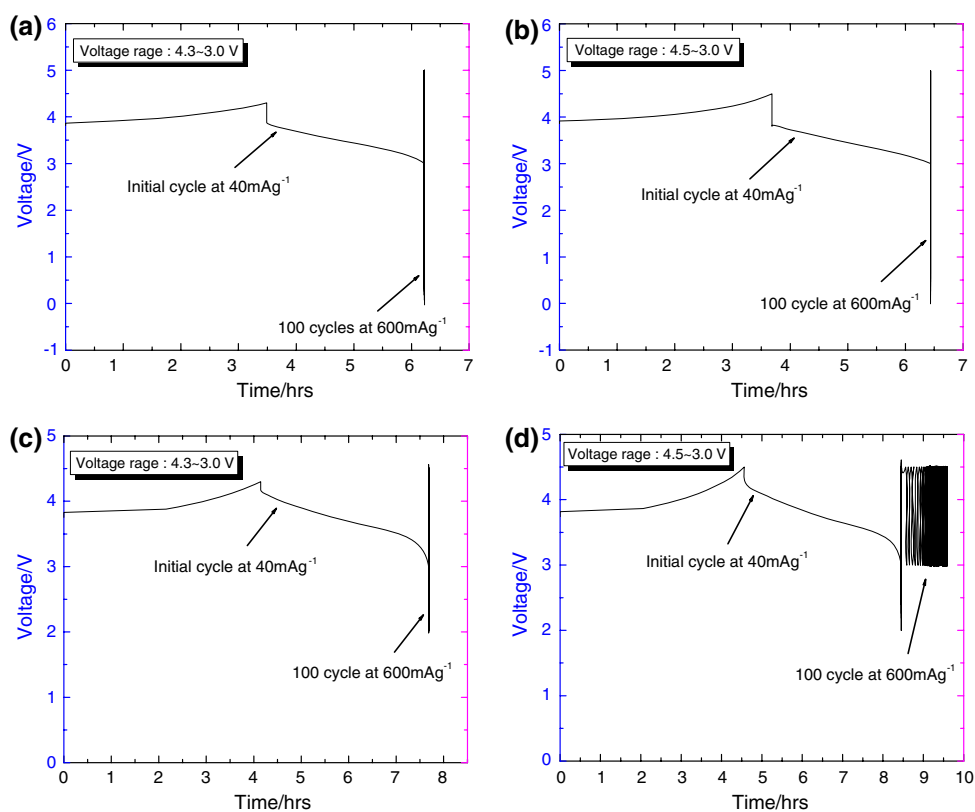
2 Experimental

$\text{LiNi}_{0.8}\text{Co}_{0.16}\text{Al}_{0.04}\text{O}_2$ used as starting material and reference samples were purchased from Sumitomo Chemical. $(\text{NH}_4)_2\text{HPO}_4$ (0.45 g) and $\text{Co}(\text{NO}_3)_2 \cdot 6\text{H}_2\text{O}$ (1.5 g) were

dissolved in distilled water for the coating solution. Ammonium hydroxide was added to the solution to increase the pH to 8.5. $\text{LiNi}_{0.8}\text{Co}_{0.16}\text{Al}_{0.04}\text{O}_2$ powder (50 g) was then slowly added to the coating solution and mixed to create a uniform slurry. The mixture was dried at 130°C for 5 h. The dried powder was ground and heat-treated at 700°C for 5 h. X-ray diffraction (XRD) patterns were obtained on the cathode electrode using a Philips X-ray diffractometer in the 2θ ranges from 15 to 70° with monochromatized $\text{Cu-K}\alpha$ radiation ($\lambda = 1.5406 \text{ \AA}$). Bare and coated samples were tested with transmission electron microscopy (TEM) (CM 20, Philips, 200 KV) before and after high current damage.

For preparation of a positive electrode, 0.15 g (3% by wt.) polyvinyl difluoride (Aldrich) was dissolved in about 12 mL of *N*-methyl-2-pyrrolidone for one hour, and then 4.75 g (94% by wt.) of sample powder and 0.15 g (3% by wt.) of Super P black (MMM Carbon Co.) were added. After 24 h of ball mill processing, the viscous slurry was coated on aluminum foil using a scalpel and dried at 90°C in an oven. The obtained cathode film was hot-pressed at 100°C . The thickness of the cathode film was about $30 \mu\text{m}$. Electrochemical cells were assembled in a dry room using the positive electrode, lithium, porous polyethylene film and 1 M LiPF_6 solution in 1:1:1 weight ratio of ethylene carbonate:dimethyl carbonate:diethyl carbonate. Cells were subjected to galvanostatic cycling using a

Fig. 1 The charge–discharge profiles of cells containing $\text{LiNi}_{0.8}\text{Co}_{0.16}\text{Al}_{0.04}\text{O}_2$ electrodes at an initial 50 mA g^{-1} and a subsequent cycling process at a current density of 600 mA g^{-1} . (a) Bare electrode, voltage range of 4.3–3.0 V; (b) bare electrode, voltage range of 4.5–3.0 V; (c) $\text{Co}_3(\text{PO}_4)_2$ -coated electrode, voltage range of 4.3–3.0 V; (d) $\text{Co}_3(\text{PO}_4)_2$ -coated electrode, voltage range of 4.5–3.0 V



Toyo (TOSCAT 3000) charge–discharge system. The impedance measurement was carried out by a impedance/grain phase analyzer (Solartron SI 1260) used in conjunction with a potentiostat (Solartron SI 1287) equipped with Z-view software, where an AC voltage with an amplitude of 5 mV was applied over the frequency range from 0.1 Hz to 100 KHz.

3 Results and discussion

A damage testing was carried out by high current cycling. The cells were initially charged and discharged at a low current rate (40 mA g^{-1}) and then cycled 100 times at a current rate of 600 mA g^{-1} for high current cycling. The voltage range was 4.3–3.0 or 4.5–3.0 V. Figure 1 shows the charge–discharge profiles of the cells containing bare and $\text{Co}_3(\text{PO}_4)_2$ -coated $\text{LiNi}_{0.8}\text{Co}_{0.16}\text{Al}_{0.04}\text{O}_2$ electrodes during high current cycling damage testing. Considering that the electrode was made with only 3% of carbon (Super P), a current density of 600 mA g^{-1} seemed to be sufficient to produce damage on the surface of the $\text{LiNi}_{0.8}\text{Co}_{0.16}\text{Al}_{0.04}\text{O}_2$ powder. In the initial charge–discharge profile before high current cycling, the bare $\text{LiNi}_{0.8}\text{Co}_{0.16}\text{Al}_{0.04}\text{O}_2$ electrode displays larger polarization than that of the $\text{Co}_3(\text{PO}_4)_2$ -coated electrode. This indicates that the coating treatment is beneficial for intercalation/deintercalation of lithium ions during cycling and decreases the internal resistance of the cells. During high current cycling, the voltage profile steeply increased and decreased. Although the voltage range was set on the cyclier to be between 4.3–3.0 or 4.5–3.0 V, the voltage profile of the bare electrode dropped below 0 V and went above 5 V. However, the $\text{Co}_3(\text{PO}_4)_2$ -coated electrode showed a relatively narrower out-of-range profile with voltages between 2 and 4.5 V. The charge and discharge capacity of the bare electrode during high current cycling was almost zero, but the $\text{Co}_3(\text{PO}_4)_2$ -coated electrode delivered capacity, even though it was very small, when high current cycling was in the voltage range of 4.5–3.0 V, which indicates that the $\text{Co}_3(\text{PO}_4)_2$ coating increased the rate capability of the $\text{LiNi}_{0.8}\text{Co}_{0.16}\text{Al}_{0.04}\text{O}_2$ electrode. The effect of the $\text{Co}_3(\text{PO}_4)_2$ coating on rate capability was reported in detail in previous work [24].

After high current cycling, the voltage profiles of the cells containing the bare and the $\text{Co}_3(\text{PO}_4)_2$ -coated electrodes were observed, as shown in Fig. 2. Initially five cycles were tested at a current density of 20 mA g^{-1} (rate of $\sim 0.1 \text{ C}$), and then the current density was increased to 40, 100, 200, 400, and 600 mA g^{-1} for subsequent cycles. The profile of the bare electrode showed high polarization even though a relatively low current density (20 mA g^{-1}) was supplied, and the profile rapidly became steeper with

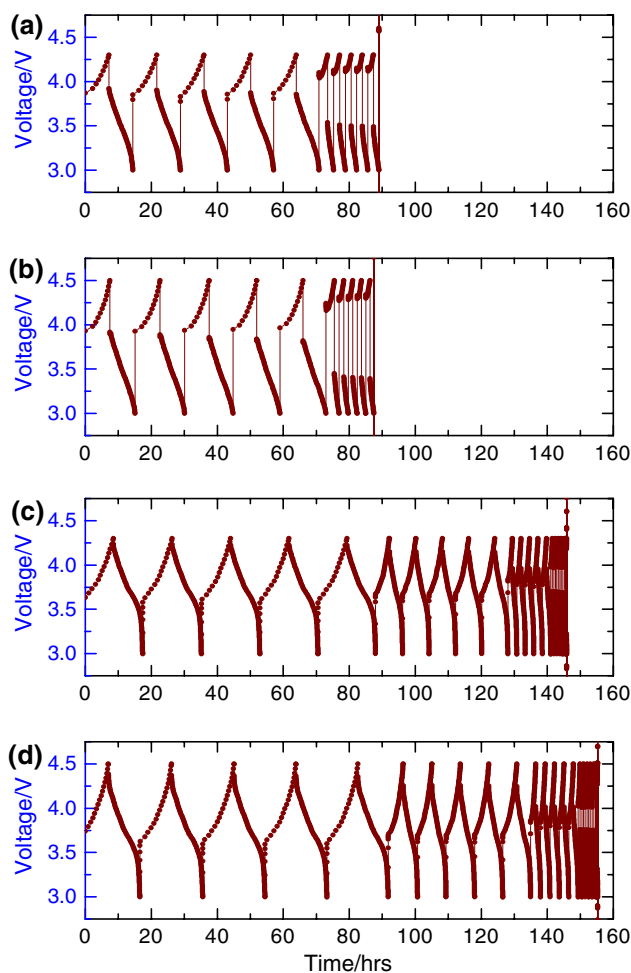


Fig. 2 Voltage profiles of cells containing $\text{LiNi}_{0.8}\text{Co}_{0.16}\text{Al}_{0.04}\text{O}_2$ electrodes after high current cycling (damage test) at different current densities. Current density of 20 mA g^{-1} for cycles 1–5, 40 mA g^{-1} for cycles 6–10, 100 mA g^{-1} for cycles 11–15, 200 mA g^{-1} for cycles 16–20, 400 mA g^{-1} for cycles 21–25, and 600 mA g^{-1} for cycles 26–30. (a) Bare electrode, measuring voltage range is 4.3–3.0 V; (b) bare electrode, measuring voltage range is 4.5–3.0 V; (c) $\text{Co}_3(\text{PO}_4)_2$ -coated electrode, measuring voltage range is 4.3–3.0 V; (d) $\text{Co}_3(\text{PO}_4)_2$ -coated electrode, measuring voltage range is 4.5–3.0 V

increasing current density. When the current density was increased over 100 mA g^{-1} , capacity dropped to almost zero. The degradation of the charge–discharge profile shows that the bare electrode was seriously damaged by high current cycling. In contrast, the polarization of the voltage profile for the $\text{Co}_3(\text{PO}_4)_2$ -coated electrode was much smaller, and the change of the profile with increasing current density was more gradual. Even though it was relatively weak, capacity was detected up to the higher current density level of 400 mA g^{-1} . Figure 3 displays the discharge capacity and cyclic performance of the cells containing bare and $\text{Co}_3(\text{PO}_4)_2$ -coated electrodes at different current densities after high current cycling (after damage testing as shown in Fig. 1). Before the high current

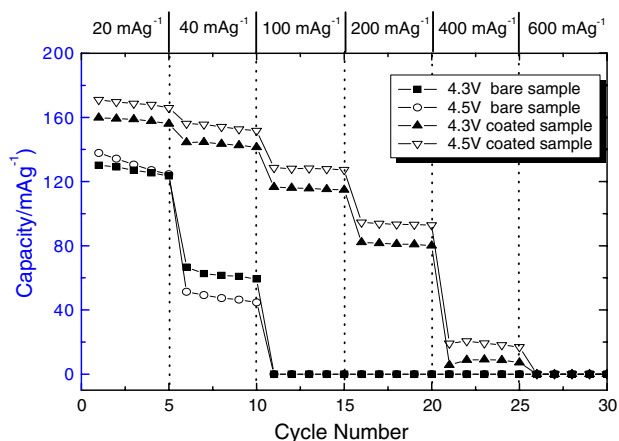


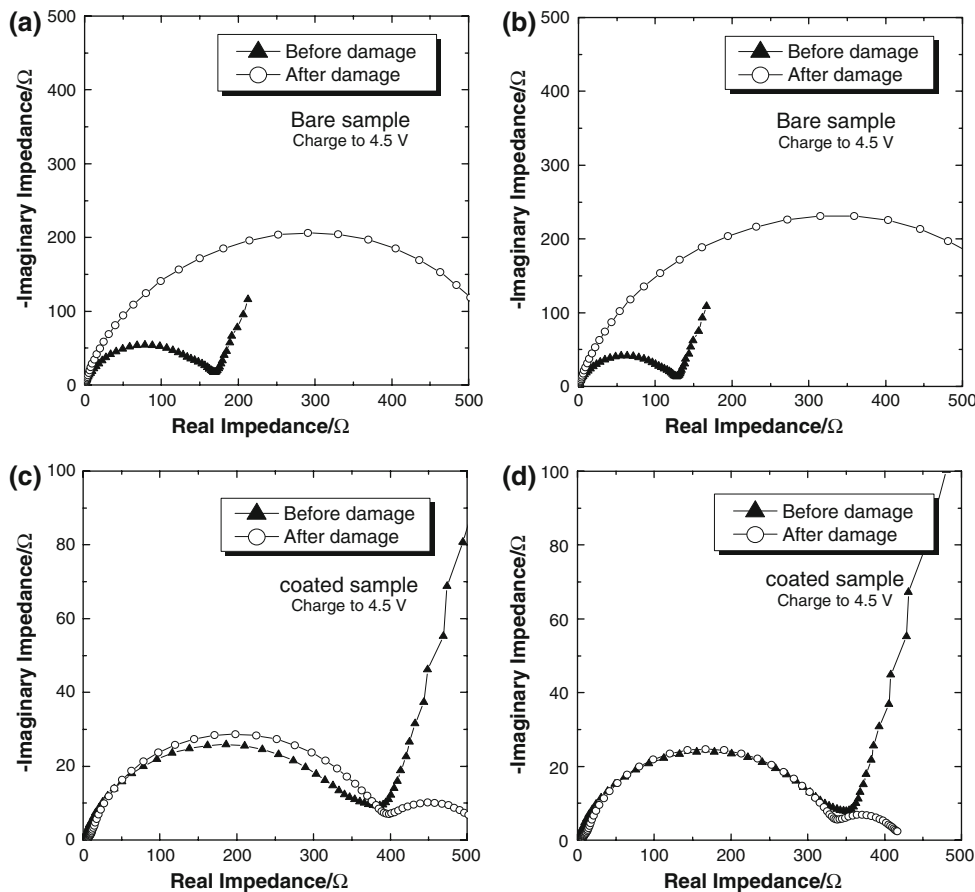
Fig. 3 The cyclic performance of cells containing bare and $\text{Co}_3(\text{PO}_4)_2$ -coated electrodes after high current cycling (damage test) at different current densities

cycling, the bare and $\text{Co}_3(\text{PO}_4)_2$ -coated electrodes exhibited a discharge capacity of ~ 190 and $\sim 200 \text{ mAh g}^{-1}$, respectively, at a current density of 20 mA g^{-1} in the voltage range of 4.5–3.0 (not included in Fig. 3) [24]. However, after high current cycling, the capacities were decreased to ~ 140 and $\sim 170 \text{ mAh g}^{-1}$ under the same

conditions, indicating both samples were damaged. However, the coated sample showed less of a capacity loss during high current cycling. With increasing current density (from 20 to 400 mA g^{-1}), the $\text{Co}_3(\text{PO}_4)_2$ -coated electrode showed higher discharge capacity and better rate capability than the bare electrode. Considering Figs. 2 and 3, it is obvious that the $\text{Co}_3(\text{PO}_4)_2$ coating can decrease damage caused by high current cycling.

AC impedance analysis has been known as a powerful technique to determine the kinetic parameters of the electrode process [25–27]. To confirm the effects of $\text{Co}_3(\text{PO}_4)_2$ coatings on $\text{LiNi}_{0.8}\text{Co}_{0.16}\text{Al}_{0.04}\text{O}_2$ electrodes, impedance spectra of the cells containing bare and coated electrodes were obtained. Figure 4 shows the Nyquist plot of the cells before and after the high current damage testing. The measurement was carried out at a charged state to 4.3 or 4.5 V. The semicircle of the Nyquist plot of the bare electrode was dramatically increased after the damage test. It is presumed that structural changes of the electrode, including chemical dissolution of the transition metal ion and/or surface film formation, may result in a remarkable increase of impedance during the damage test. In contrast, it is interesting that the size of the semicircle for the

Fig. 4 Nyquist plot of cells containing $\text{LiNi}_{0.8}\text{Co}_{0.16}\text{Al}_{0.04}\text{O}_2$ electrodes before and after damage testing. (a) Bare electrode, charged to 4.3 V; (b) bare electrode, charged to 4.6 V; (c) $\text{Co}_3(\text{PO}_4)_2$ -coated electrode, charged to 4.3 V; (d) $\text{Co}_3(\text{PO}_4)_2$ -coated electrode, charged to 4.5 V



$\text{Co}_3(\text{PO}_4)_2$ -coated electrode did not increase; instead, another small semicircle appeared during the damage test.

The electrochemical reaction of the positive electrode proceeds as an insertion/extraction reaction of lithium ions, which leads to changes in the molar volume of the materials. Thus, the reaction induces mechanical stress and strain to the oxide particles [28]. As the current density is increased during cycling, the stress and strain will increase due to rapid diffusion of lithium ions between the cathode electrode and the electrolyte, which can lead to damage of the electrode, such as structural changes or chemical decomposition/dissolution of the metal oxide. Specifically, the damage will focus on the surface of the powder because it is contacting and reacting with the electrolyte. The vulnerable surface of the electrode could be protected by a nanoparticle $\text{Co}_3(\text{PO}_4)_2$ coating. $\text{Co}_3(\text{PO}_4)_2$ nanoparticles were reported to have completely diffused into the surface of the cathode material and reacted with lithium of the cathode material or a surface impurity, such as Li_2CO_3 [10]. As such, it is expected that the surface of $\text{Co}_3(\text{PO}_4)_2$ -coated $\text{LiNi}_{0.8}\text{Co}_{0.15}\text{Al}_{0.05}\text{O}_2$ powder would be covered with Li_xCoPO_4 phase [12, 24]. It is obvious that the Li_xCoPO_4 phase can effectively prevent structural changes or chemical decomposition/dissolution of the metal oxide [12], thus maintaining low impedance during high current damage testing. Moreover, the covalent-bond nature of $(\text{PO}_4)^{3-}$ with its cation contributed to a strong resistance toward reaction with the electrolyte [8]. However, a new small semicircle was formed in the very low frequency range after the damage test, which may be associated with a new impedance factor originating from a surface reaction between the surface coating layer and the electrolyte during the high current cycling process. As shown in Figs. 2 and 3, the capacity and charge retention of the $\text{Co}_3(\text{PO}_4)_2$ -coated electrode was deteriorated after the damage test, although it was less serious than the deterioration of the bare electrode. The new semicircle can explain the degradation of the electrochemical properties of the $\text{Co}_3(\text{PO}_4)_2$ -coated electrode after the damage test.

The phases of bare and $\text{Co}_3(\text{PO}_4)_2$ -coated $\text{LiNi}_{0.8}\text{Co}_{0.16}\text{Al}_{0.04}\text{O}_2$ powders were investigated by XRD analysis, as shown in Fig. 5. The XRD patterns of both samples after damage testing are identical to those of samples before damage testing. Even though, specifically in the case of bare $\text{LiNi}_{0.8}\text{Co}_{0.16}\text{Al}_{0.04}\text{O}_2$ powder, it is possible that there could be formation of a surface layer, structural phase transformation, or dissolution of cation ions, they were not detected by XRD analysis. The damage of $\text{LiNi}_{0.8}\text{Co}_{0.16}\text{Al}_{0.04}\text{O}_2$ powder during high current cycling must occur only on the surface of the electrode, such that it is not enough to detect by XRD analysis. Herein, a TEM analysis was introduced to investigate the surface morphology of

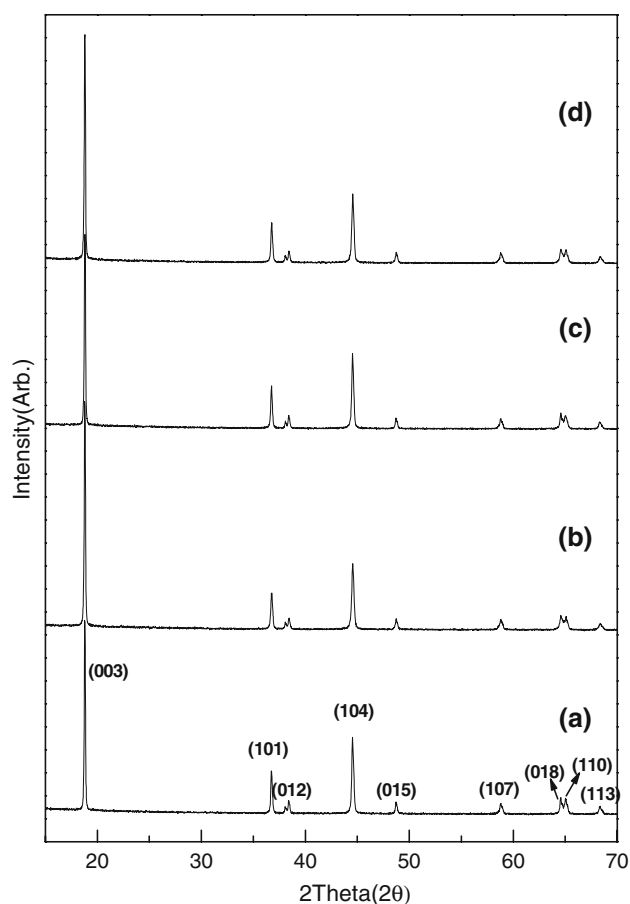
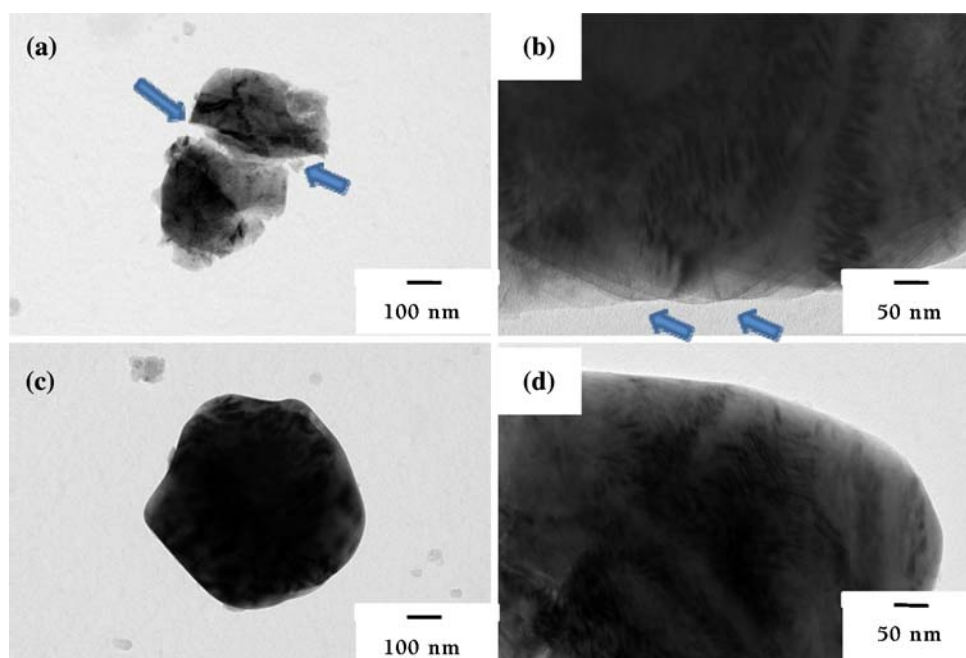


Fig. 5 XRD patterns of $\text{LiNi}_{0.8}\text{Co}_{0.16}\text{Al}_{0.04}\text{O}_2$ powder. (a) Bare powder, before the damage test; (b) $\text{Co}_3(\text{PO}_4)_2$ -coated powder, before the damage test; (c) bare powder, after the damage test; (d) $\text{Co}_3(\text{PO}_4)_2$ -coated powder, after the damage test

$\text{LiNi}_{0.8}\text{Co}_{0.16}\text{Al}_{0.04}\text{O}_2$ powder in detail after the damage test. Figure 6 displays the bright field TEM images of $\text{LiNi}_{0.8}\text{Co}_{0.16}\text{Al}_{0.04}\text{O}_2$ primary particles after the high current damage test. Some bare particles showed unstable features containing microcracks and other extended defects on the surface. Figure 6a shows highly strained particles in which microcracks are clearly visible (indicated by arrows). Approximately 20–30% of particles appeared to have some sign of damage, which must have originated due to strain from rapid lattice expansion/extraction during high current cycling. In contrast, most of the $\text{Co}_3(\text{PO}_4)_2$ -coated particles displayed clear surfaces and unchanged features during high current cycling. Even though some particles had extended defects on their surface, it was a much smaller amount when compared with that of bare particles. The TEM analysis indicates that the $\text{Co}_3(\text{PO}_4)_2$ treatment is a very effective method to decrease surface damage developed during damage testing, thus it can reduce capacity loss during high current cycling.

Fig. 6 Bright field TEM images of $\text{LiNi}_{0.8}\text{Co}_{0.16}\text{Al}_{0.04}\text{O}_2$ powder after damage testing. (a) Bare powder, arrows show microcracks; (b) bare powder, arrow shows extended defects; (c and d) $\text{Co}_3(\text{PO}_4)_2$ -coated powder



4 Conclusions

$\text{Co}_3(\text{PO}_4)_2$ coating on $\text{LiNi}_{0.8}\text{Co}_{0.15}\text{Al}_{0.05}\text{O}_2$ powder successfully suppressed damage due to high current cycling. Damage to electrodes, including degradation of capacity and rate performance, following high current cycling were improved by a $\text{Co}_3(\text{PO}_4)_2$ coating. Based on impedance and TEM analysis, it can be concluded that $\text{Co}_3(\text{PO}_4)_2$ coatings effectively prevent an increase in impedance and reduce the generation of cracks and other extended defects during high current damage testing, thereby resulting in less degradation of the electrochemical properties of $\text{Co}_3(\text{PO}_4)_2$ -coated electrodes.

Acknowledgements This work was supported by the Division of advanced batteries in NGE program (Project No. 10016454).

References

1. Cho J, Kim YJ, Kim TJ, Park B (2001) *Angew Chem Int Ed Engl* 40:3367
2. Cho J, Kim YJ, Park B (2000) *Chem Mater* 12:3788
3. Cho J, Lee JG, Kim B, Park B (2003) *Chem Mater* 15:3190
4. Cho J, Kim YJ, Park B (2001) *J Electrochem Soc* 148:A1110
5. Zhang ZR, Liu HS, Gong ZL, Yang Y (2004) *J Electrochem Soc* 151:A599
6. Cho J (2003) *Electrochem Commun* 5:146
7. Kim YJ, Kim H, Kim B et al (2003) *Chem Mater* 15:1505
8. Cho J, Kim H, Park B (2004) *J Electrochem Soc* 151:A1707
9. Amine K, Yasuda H, Yamachi M (2000) *Electrochem Solid State Lett* 3:178
10. Lee H, Kim MG, Cho J (2007) *Electrochem Commun* 9:149
11. Gao G (2004) *Nanostructures and nanomaterials*. World Science Publishing Co. Ltd., Singapore
12. Kim Y, Cho J (2007) *J Electrochem Soc* 154:A495
13. Saadouni I, Delmas C (1998) *J Solid State Chem* 136:8
14. Li W, Reimers JN, Dahn JR (1993) *Solid State Ion* 67:123
15. Nishida Y, Nakane K, Satoh T (1997) *J Power Sources* 68:561
16. Omand H, Brousse T, Marhic C, Schleich DM (2004) *J Electrochem Soc* 151:A922
17. Belharouak I, Lu W, Vissers D, Amine K (2006) *Electrochem Commun* 8:329
18. Shaju KM, SubbaRao GV, Chowdari BVR (2004) *J Electrochem Soc* 151:A1324
19. Kim J, Hong Y, Ryu KS, Kim MG, Cho J (2006) *Electrochem Solid State Lett* 9:A19
20. Liu HS, Zhang ZR, Gong ZL, Yang Y (2004) *Electrochem Solid State Lett* 7:A190
21. Matsumoto K, Kuzuo R, Takeya K, Yamanaka A (1999) *J Power Sources* 81–82:558
22. Liang HY, Qiu XP, Chen HL, He ZQ, Zhu WT, Chen LQ (2004) *Electrochem Commun* 6:789
23. Abraham KM, Pasquariello DM, Willstaedt EM (1998) *J Electrochem Soc* 145:482
24. Ryu KS, Lee SH, Kwak D, Kim J, Cho J, Park YJ (2007) *Materials Chemistry and Physics* submitted
25. Troltzsch U, Kanoun O, Trankler H (2006) *Electrochim Acta* 51:1664
26. Zhou W, Bao S, He B, Liang Y, Li H (2006) *Electrochimica Acta* 51:4701
27. Mohamedi M, Takahashi D, Itoh T, Umeda M, Uchida I (2002) *J Electrochem Soc* 149:A19
28. Vetter J, Novak P, Wagner MR et al (2005) *J Power Sources* 147:269